A Distributed Positioning Algorithm for Cooperative Active and Passive Sensors

Mohammad Reza Gholami[†], Sinan Gezici[♯], Mats Rydström[†], and Erik G. Ström[†]

† Chalmers University of Technology, Department Signals and Systems, Gothenburg, Sweden

♯ Bilkent University, Department of Electrical and Electronics Engineering, Ankara, Turkey

Abstract—**The problem of positioning a target node is studied for wireless sensor networks with cooperative active and passive sensors. Two-way time-of-arrival and time-difference-of-arrival measurements made by both active and passive nodes are used to estimate the position of the target node. A maximum likelihood estimator (MLE) can be employed to solve the problem. Due to the nonlinear nature of the cost function in the MLE, an iterative search might converge to local minima which often results in large estimation errors. To avoid this drawback, we instead formulate the problem of positioning as finding the intersection of a number of convex sets derived from measurements. To obtain this intersection, we apply the *projection onto convex sets* approach, which is robust and can be implemented in a distributed manner. Simulations are performed to compare the performance of the MLE and the proposed method.**

Index Terms– Cooperative positioning, projection onto convex sets, wireless sensor networks.

I. INTRODUCTION

Nowadays wireless sensor networks (WSNs) have been considered for many civil and military applications. Accurate positioning of the sensor nodes in a WSN is often necessary in order for the WSN to be able to function as intended [1]. Most studies in the literature assume that there are some reference nodes, also called anchor nodes, that can be used to estimate the position of a target node [2], [3]. In general, there are various positioning algorithms based on time-of-arrival (TOA), time-difference-of-arrival (TDOA), received signal-strength (RSS), and angle-of-arrival that can be used in different applications [4].

Two-way TOA (TW-TOA) has been considered as an effective approach in the literature (e.g., [5]), mainly because of its relatively high accuracy and lack of synchronization requirements. In this approach, a reference node sends a signal to a target node, and waits for a response from it. The round-trip time delay between the reference node and the target node gives an estimate of the distance between them. As the number of reference nodes in a WSN increases, the position of the target node can be estimated more accurately via TW-TOA estimation. Since, in practice, there are some limitations on increasing the number of reference nodes due to power and complexity constraints, the idea of cooperation between reference nodes is proposed in [6] to decrease the number of transmissions, and its theoretical analysis is presented in

[5]. In this method, some reference nodes, called primary reference nodes (PRNs), initiate range estimation by sending a signal. The target replies to received signals by sending an acknowledgement. Suppose that there are some other reference nodes, which can listen to both signals, and are called as secondary reference nodes (SRNs). It has been shown that the SRNs can help the PRNs to estimate the target position more accurately [5]. In fact, it is possible to get the same performance with fewer PRNs when measurements from the SRNs are involved in the positioning process. In this model, the PRNs are active nodes and the SRNs play the role of passive nodes (i.e., they just listen to the signals between the target and the PRNs). The model considered here is based on cooperation between active and passive reference nodes, which is different from targets' cooperation in a cooperative network [7].

In this paper, it is assumed that the SRNs are able to receive signals from both the target and the PRNs. Therefore, the SRNs are able to measure the TDOA between the target signal and the signals of the PRNs. In this case, a maximum likelihood estimator (MLE) derived in [5] can be employed to improve positioning accuracy compared to the non-cooperative approach. However, due to the nonlinear nature of the cost function in the MLE, an iterative search may converge to local minima which often results in large estimation errors. Using a geometric interpretation, we instead formulate the positioning problem as finding the intersection of a number of convex sets obtained from the TW-TOA and TDOA measurements in SRNs and PRNs. Successive orthogonal projections onto discs and elliptical sets are employed to solve the optimization problem of cooperative positioning. The proposed algorithm is robust and converges after a few iterations. The nature of the algorithm makes it suitable for a distributed implementation in a WSN.

The remainder of the paper is organized as follows. Sec. II explains the signal model considered in this paper. The positioning algorithms are explained in Sec. III and simulation results are discussed in Sec. IV. Finally, Sec. V makes some concluding remarks.

II. SIGNAL MODEL

Let us consider a two-dimensional network[1] with $N + M$ reference nodes located at known positions, $\mathbf{z}_i = [x_i, y_i]^T \in$

---

[1]The generalization to a three-dimensional scenario is straightforward, but is not explored here.

$\mathbb{R}^2$, $i = 1, ..., N + M$. Suppose that N PRNs are used to measure the TW-TOA between the PRNs and the target to be located, and that M SRNs are able to listen and measure signals transmitted by the PRNs and the target. For simplicity, we assume that the first N sensors are the primary nodes, and the remaining M sensors are the secondary nodes.

Let us define $\mathcal{C} = \{(i, j) : i = 1, ..., N, j = N + 1, ..., N + M\}$ as the set of all pairs with one active and one passive sensor which are connected. The TW-TOA measurement between reference node i and the target, located at coordinates $\boldsymbol{\theta} = [x, y]^T \in \mathbb{R}^2$, can be written as [5]

$$\hat{t}_i = \frac{r_i(\boldsymbol{\theta})}{c} + \frac{n_{T,i}}{2} + \frac{n_{i,T}}{2} , \quad i = 1, ..., N, \quad (1)$$

where c is the propagation speed of light, $r_i(\boldsymbol{\theta}) = \|\mathbf{z}_i - \boldsymbol{\theta}\|$ is the distance between the ith PRN and the point $\boldsymbol{\theta}$, $n_{i,T}$ is the TOA estimation error at the target node for the signal transmitted from the ith PRN, and $n_{T,i}$ is the TOA estimation at the ith PRN for the signal transmitted from the target node. The estimation errors are modeled as zero-mean Gaussian random variables with variances $\sigma_{T,i}^2$ and $\sigma_{i,T}^2$; i.e., $n_{T,i} \sim \mathcal{N}(0, \sigma_{T,i}^2)$ and $n_{i,T} \sim \mathcal{N}(0, \sigma_{i,T}^2)$ [5].

Suppose that the SRNs are able to measure the TOA based on the received signal from the target and the PRNs. The TOA estimate of the ith PRN in the jth SRN is

$$\hat{t}_{i,j} = T_{o_i} + \frac{r_{i,j}}{c} + n_{i,j} , \quad (i, j) \in \mathcal{C}, \quad (2)$$

where the ith PRN sends its signal at time instant T_{o_i}, that is unknown to the SRN, and $n_{i,j}$ is modeled as a Gaussian random variable $n_{i,j} \sim \mathcal{N}(0, \sigma_{i,j}^2)$. Suppose that the response signal from the target to this signal is also received by the jth SRN. The TOA estimate for this signal is given by

$$\hat{t}_{i,T,j} = T_{o_i} + \frac{r_i(\boldsymbol{\theta})}{c} + \frac{r_j(\boldsymbol{\theta})}{c} + n_{i,T} + n_{T,j} , \quad (i, j) \in \mathcal{C}. \quad (3)$$

Having these two measurements in the SRN, namely, measurement in (2) and in (3), we are able to measure the TDOA between the ith PRN and the target which corresponds to the distance from the ith PRN to the target plus the distance from the target to the jth SRN.

III. POSITIONING ALGORITHMS

In this section we propose an iterative algorithm to extract position information based on measurements collected by the PRNs and SRNs. To gain some insight into the problem, let us consider Fig. 1, where one PRN performs TW-TOA estimation with the target. Namely, the PRN sends a signal to the target, and the target replies to this signal. Here, we assume that the turn-around time in the target is extremely small; Hence, it can be neglected. Suppose that two other nodes (SRN1 and SRN2) listen to both signals. Since the distances between the reference nodes are known, it is possible in the secondary node to estimate the time reference from (2); Hence, the SRNs are able to estimate the overall distance from the PRN to the target
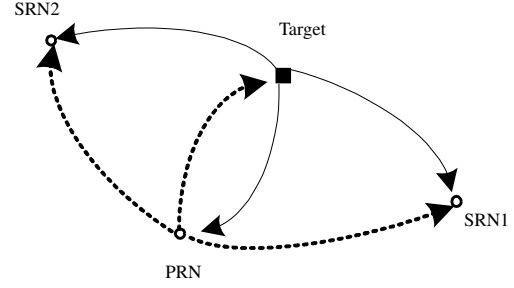

Fig. 1: A primary node initiates positioning by transmitting a signal to the target whereupon the target replies to the received signal. Both signals are received in the secondary nodes.

and the target to the SRN as follows:

$$\hat{r}_{i,T,j} = c(\hat{t}_{i,T,j} - \hat{T}_{o_i})$$
$$= r_i(\boldsymbol{\theta}) + r_j(\boldsymbol{\theta}) + c\,n_{j,T} + c\,n_{i,T} - c\,n_{i,j}, \quad (i, j) \in \mathcal{C}, \quad (4)$$

where $\hat{T}_{o_i}$ is an estimate of T_{o_i}. From (1), the distance estimate to the target in the ith PRN is expressed as

$$\hat{r}_i = c\,\hat{t}_i = r_i(\boldsymbol{\theta}) + \frac{c}{2}n_{i,T} + \frac{c}{2}n_{T,i} , \quad i = 1, ..., N. \quad (5)$$

It is observed that there is correlation between the TW-TOA and the TDOA measurements in the PRNs and SRNs. Considering all the collected measurements in both the PRNs and SRNs, the MLE can be obtained as [5]

$$\hat{\boldsymbol{\theta}} = \arg\min_{\boldsymbol{\theta}} \sum_{i=1}^{N} \left\{ \left(\frac{2}{\sigma_i^2} - \frac{1}{s_i \sigma_i^4} \right) (\hat{r}_i - r_i(\boldsymbol{\theta}))^2 \right.$$
$$- \frac{1}{s_i} \left(\sum_{j=N+1}^{M+N} \frac{\hat{r}_{i,T,j} - r_i(\boldsymbol{\theta}) - r_j(\boldsymbol{\theta})}{4\sigma_j^2} \right)^2$$
$$- \frac{\hat{r}_i - r_i(\boldsymbol{\theta})}{s_i \sigma_i^2} \sum_{j=N+1}^{N+M} \frac{(\hat{r}_{i,T,j} - r_i(\boldsymbol{\theta}) - r_j(\boldsymbol{\theta}))}{2\sigma_j^2}$$
$$\left. + \sum_{j=N+1}^{N+M} \frac{(\hat{r}_{i,T,j} - r_i(\boldsymbol{\theta}) - r_j(\boldsymbol{\theta}))^2}{2\sigma_j^2} \right\}, \quad (6)$$

where

$$s_i \triangleq \frac{1}{2\sigma_T^2} + \frac{1}{2\sigma_i^2} + \sum_{j=N+1}^{M+N} \frac{1}{4\sigma_j^2} . \quad (7)$$

Due to the nonlinear nature of the cost function in (6), an iterative search may converge to local minima, resulting in large estimation errors. In the sequel, using a geometric interpretation of the problem, we propose an iterative method to estimate the target position.

Initially, suppose that there is no noise in the TOA estimation based on the TW-TOA measurement. Then, it is clear that the target can be found on a circle with radius r_i centered around $\mathbf{z}_i$. Similarly, a TDOA measurement made by an SRN defines an ellipse with foci $\mathbf{z}_i$ and $\mathbf{z}_j$ on which the target is located. In absence of noise, the target position can be found in the intersection of a number of circles and a number of

ellipses. For the ith PRN and distance estimate $\hat{r}_i$, consider the disc

$$\mathcal{D}_i = \{\boldsymbol{\theta} \in \mathbb{R}^2 : r_i(\boldsymbol{\theta}) \leq \hat{r}_i\} , \tag{8}$$

and for the ith SRN and the jth PRN and distance $\hat{r}_{i,T,j}$, define the elliptic set $\mathcal{E}_l$

$$\mathcal{E}_l = \{\boldsymbol{\theta} \in \mathbb{R}^2 : r_i(\boldsymbol{\theta}) + r_j(\boldsymbol{\theta}) \leq \hat{r}_{i,T,j}\} . \tag{9}$$

Now, the target can be found in the intersection of sets $\mathcal{D}_i$, $i = 1, ..., N$ and $\mathcal{E}_l$, $l = 1, ..., NM$. Hence the proposed estimator is

$$\hat{\boldsymbol{\theta}} \in \mathcal{J} = \bigcap_{i=1}^{N(1+M)} \mathcal{J}_i , \tag{10}$$

where $\mathcal{J}_i = \mathcal{D}_i$ for $i \leq N$ and $\mathcal{J}_i = \mathcal{E}_i$ if $i > N$. For the case of an empty intersection, which can occur for instance due to the measurement noise, the estimator finds a point that minimizes the sum of squared distances to the sets $\mathcal{J}_i$, $i = 1, ..., N(1 + M)$, that is,

$$\hat{\boldsymbol{\theta}} = \arg\min_{\boldsymbol{\theta}} \sum_{i=1}^{N(1+M)} \|\boldsymbol{\theta} - \mathcal{P}_{\mathcal{J}_i}(\boldsymbol{\theta})\|^2 , \tag{11}$$

where $\mathcal{P}_{\mathcal{J}_i}(\boldsymbol{\theta})$ is the orthogonal projection of $\boldsymbol{\theta}$ onto convex set $\mathcal{J}_i$. For a disc with radius $\hat{r}_i$, the projection function is defined as follows:

$$\mathcal{P}_{\mathcal{J}_i}(\boldsymbol{\theta}) = \begin{cases} \boldsymbol{\theta} , & \text{if } r_i(\boldsymbol{\theta}) \leq \hat{r}_i \\ \frac{\boldsymbol{\theta} - \mathbf{z}_i}{\|\boldsymbol{\theta} - \mathbf{z}_i\|} \hat{r}_i , & \text{otherwise.} \end{cases} \tag{12}$$

For an elliptic set, we need to project a point onto an ellipse. Here we consider a geometric solution to the elliptic projection problem. A general form of an ellipse can be expressed as

$$Ax^2 + 2Bxy + Cy^2 + 2Dx + 2Ey + F = 0 . \tag{13}$$

The parameters (A, B, C, D, E and F) of an ellipse can be obtained versus known positions of the reference nodes and the distance estimates to the target. In the absence of noise in the TOA measurements, for primary node i and secondary node j, we obtain the following relation from (4):

$$r_i(\boldsymbol{\theta}) + r_j(\boldsymbol{\theta}) = r_{i,T,j} = \|\mathbf{z}_i - \boldsymbol{\theta}\| + \|\mathbf{z}_j - \boldsymbol{\theta}\| . \tag{14}$$

Moving one term of (14) to the left-hand-side and squaring both sides, we have

$$\|\mathbf{z}_i - \boldsymbol{\theta}\|^2 = r_{i,T,j}^2 - 2r_{i,T,j}\|\mathbf{z}_j - \boldsymbol{\theta}\| + \|\mathbf{z}_j - \boldsymbol{\theta}\|^2 . \tag{15}$$

With some similar manipulations, we obtain

$$4r_{i,T,j}^2((x - x_i)^2 + (y - y_i)^2) = a^2 x^2 + b^2 y^2 + d^2 + 2adx + 2bdy + 2abxy , \tag{16}$$

where $a = 2(x_i - x_j)$, $b = 2(y_i - y_j)$, and $d = x_j^2 - x_i^2 + y_j^2 - y_i^2$. Finally, the general form of the ellipse becomes

$$(a^2 - 4r_{i,T,j}^2)x^2 + 2abxy + (b^2 - 4r_{i,T,j}^2)y^2 + 2(ad + 4r_{i,T,j}^2 x_i)x + 2(bd + 4r_{i,T,j}^2 y_i)y + d^2 - 4r_{i,T,j}^2(x_i^2 + y_i^2) = 0. \tag{17}$$

Therefore, the parameters A, B, C, D, E and F can be computed from (17). Equation (13) can be written in a matrix form as

$$\mathbf{z}^T \mathbf{M} \mathbf{z} = 0 , \tag{18}$$

where $\mathbf{z} = [x \; y \; 1]^T$ and the symmetric matrix $\mathbf{M} \in \mathbb{R}^3$ is defined as follows:

$$\mathbf{M} = \begin{bmatrix} A & B & D \\ B & C & E \\ D & E & F \end{bmatrix} . \tag{19}$$

To project a point onto an ellipse, we first find a transform that transforms the ellipse into a unit circle. We subject the point to this transform, project onto the unit circle, and subject the projected point to the inverse transform. A unit circle can be expressed as

$$\tilde{\mathbf{z}}^T \mathbf{I}_{-1} \tilde{\mathbf{z}} = 0 , \tag{20}$$

where the diagonal matrix $\mathbf{I}_{-1}$ is

$$\mathbf{I}_{-1} = \begin{bmatrix} 1 & 0 & 0 \\ 0 & 1 & 0 \\ 0 & 0 & -1 \end{bmatrix} . \tag{21}$$

Now, we try to find a function that transforms the ellipse (18) to a unit circle (20). In general every ellipse can be obtained by translating, rotating and scaling a unit circle, i.e., through transform function $\mathbf{F} = \mathbf{TRS}$ [8]. Matrices $\mathbf{S}$, $\mathbf{R}$ and $\mathbf{T}$ are defined as follows:

$$\mathbf{S} = \begin{bmatrix} s_{1,1} & 0 & 0 \\ 0 & s_{2,2} & 0 \\ 0 & 0 & 1 \end{bmatrix} = \begin{bmatrix} \mathbf{S}_{2\times 2} & \mathbf{0} \\ \mathbf{0}^T & 1 \end{bmatrix}, \tag{22}$$

where $\mathbf{0} = [0, 0]^T$,

$$\mathbf{R} = \begin{bmatrix} \cos\alpha & -\sin\alpha & 0 \\ \sin\alpha & \cos\alpha & 0 \\ 0 & 0 & 1 \end{bmatrix} = \begin{bmatrix} \mathbf{R}_{2\times 2} & \mathbf{0} \\ \mathbf{0} & 1 \end{bmatrix}, \tag{23}$$

and [2]

$$\mathbf{T} = \begin{bmatrix} 1 & 0 & x_c \\ 0 & 1 & y_c \\ 0 & 0 & 1 \end{bmatrix} = \begin{bmatrix} \mathbf{I}_{2\times 2} & \mathbf{z}_c^T \\ \mathbf{0} & 1 \end{bmatrix}, \tag{24}$$

where $\mathbf{z}_c = [x_c, y_c]^T$ is the center of the ellipse. Now the relation between the ellipse and a unit circle can be expressed as $\mathbf{z} = \mathbf{F}\tilde{\mathbf{z}}$. To find the matrices $\mathbf{T}, \mathbf{R}$ and $\mathbf{S}$, we replace the inverse transform of $\mathbf{F}$ in (20) and compare with (18) to yield

$$\mathbf{M} = (\mathbf{TRS})^{-T} \mathbf{I}_{-1} (\mathbf{TRS})^{-1}, \tag{25}$$

After some manipulations we get [8]

$$\mathbf{M} = \begin{bmatrix} \mathbf{R}_{2\times 2}\mathbf{S}_{2\times 2}^{-2}\mathbf{R}_{2\times 2}^T & -\mathbf{R}_{2\times 2}\mathbf{S}_{2\times 2}^{-2}\mathbf{R}_{2\times 2}^T\mathbf{z}_c \\ -\mathbf{z}_c^T\mathbf{R}_{2\times 2}\mathbf{S}_{2\times 2}^{-2}\mathbf{R}_{2\times 2}^T & \mathbf{z}_c^T\mathbf{R}_{2\times 2}\mathbf{S}_{2\times 2}^{-2}\mathbf{R}_{2\times 2}^T\mathbf{z}_c \end{bmatrix} . \tag{26}$$

To find the transformed matrix, it is enough to find sub-matrices $\mathbf{R}_{2\times 2}$ and $\mathbf{S}_{2\times 2}^{-2}$. Since matrix $\mathbf{M}$ is symmetric, we

---

[2] In this paper, $\mathbf{A}_{m\times n}$, in general, denotes the upper left $m \times n$ part of $\mathbf{A}$.
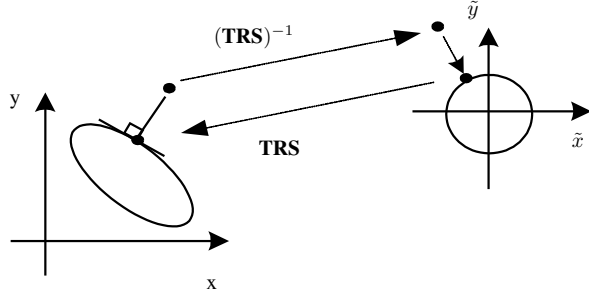
Fig. 2: Projection of a point onto an ellipse

can use the singular value decomposition technique for the upper left 2×2 matrix of $\mathbf{M}$, i.e.,

$$\mathbf{M}_{2 \times 2} = \mathbf{U}^T \boldsymbol{\lambda} \mathbf{U} = \mathbf{R}_{2 \times 2} \mathbf{S}_{2 \times 2}^{-2} \mathbf{R}_{2 \times 2}^T . \tag{27}$$

It is clear that $\mathbf{R}_{2 \times 2} = \mathbf{U}^T$. To find the scaling matrix, (25) can be written based on the scaling matrix,

$$\mathbf{S}^{-T} \mathbf{I}_{-1} \mathbf{S}^{-1} = \begin{bmatrix} \frac{1}{s_{1,1}^2} & 0 & 0 \\ 0 & \frac{1}{s_{2,2}^2} & 0 \\ 0 & 0 & -1 \end{bmatrix} = (\mathbf{TR})^T \mathbf{M} (\mathbf{TR}). \tag{28}$$

Finally, the projection of a point $\boldsymbol{\theta}$ outside of an ellipse onto the ellipse can be performed as follows:

1) Compute the transform function $\mathbf{F} = (\mathbf{TRS})^{-1}$.
2) Transform the point to the new coordinate, where the ellipse is transformed to the unit circle, i.e. $\boldsymbol{\theta}_T = \left[\mathbf{F} \begin{bmatrix} \boldsymbol{\theta} \\ 1 \end{bmatrix} \right]_{2 \times 1}$.
3) Find the projection of $\boldsymbol{\theta}_T$ onto the unit circle, $\mathcal{P}(\boldsymbol{\theta}_T) = \boldsymbol{\theta}_T / \|\boldsymbol{\theta}_T\|$.
4) In the final step, using the inverse transform $\mathbf{F}^{-1} = \mathbf{TRS}$, transform the projected point on the unit circle to a point on the ellipse, i.e, $\mathcal{P}(\boldsymbol{\theta}) = \left[\mathbf{F}^{-1} \begin{bmatrix} \mathcal{P}(\boldsymbol{\theta}_T) \\ 1 \end{bmatrix} \right]_{2 \times 1}$.

Fig. 2 shows how a point outside of an ellipse is projected onto the ellipse.

To find the position of the target, we employ orthogonal projection onto convex sets (POCS). In the non-cooperative case, POCS is applied to a number of discs derived by the PRNs (C-POCS), while for the cooperative case, it is applied to both circular and elliptical sets (CE-POCS). Algorithm 1 shows one type of CE-POCS implementation where POCS is sequentially applied to circular and elliptical sets (CE-POCS1). We also suggest a different type of CE-POCS implementation in the following.

Since there are two different convex sets derived from different measurements, circular and elliptical sets, one method of implementing CE-POCS is to apply POCS to circular and elliptical sets individually, i.e., orthogonal projection onto circular convex set and orthogonal projection onto elliptical

---

Algorithm 1 CE-POCS1

1: Initialization $\boldsymbol{\theta}^0$ is arbitrary
2: **for** $k = 0$ until convergence **do**
3:     $\nu(k) \Longleftarrow$ k mod $N(1 + M)$
4:     **if** $\boldsymbol{\theta}^k \in \mathcal{I}_{\nu(k)}$ **then**
5:        $\boldsymbol{\theta}^{k+1} \Longleftarrow \boldsymbol{\theta}^k$
6:     **else**
7:        **if** $\nu(k) \leq N$ **then**
8:           $\mathcal{P}_{\mathcal{I}_{\nu(k)}}(\boldsymbol{\theta}^k) \Longleftarrow \frac{\boldsymbol{\theta}^k - \mathbf{z}_{\nu(k)}}{\|\boldsymbol{\theta}^k - \mathbf{z}_{\nu(k)}\|} \hat{r}_{\nu(k)}$
9:        **else**
10:           $\boldsymbol{\theta}_T \Longleftarrow \left[\mathbf{F}_{\nu(k)} \begin{bmatrix} \boldsymbol{\theta}^k \\ 1 \end{bmatrix} \right]_{2 \times 1}$
11:           $\mathcal{P}_{\mathcal{I}_{\nu(k)}}(\boldsymbol{\theta}^k) \Longleftarrow \left[\mathbf{F}_{\nu(k)}^{-1} \begin{bmatrix} \frac{\boldsymbol{\theta}_T}{\|\boldsymbol{\theta}_T\|} \\ 1 \end{bmatrix} \right]_{2 \times 1}$
12:        **end if**
13:        $\boldsymbol{\theta}^{k+1} \Longleftarrow (1 - \lambda_k)\boldsymbol{\theta}^k + \lambda_k \mathcal{P}_{\mathcal{I}_{\nu(k)}}(\boldsymbol{\theta}^k)$
14:     **end if**
15: **end for**

Algorithm 2 CE-POCS2

1: Initialization $\boldsymbol{\theta}_p^0$ and $\boldsymbol{\theta}_s^0$ are arbitrary
2: **for** k $= 0$ until convergence **do**
3:     **for** $l = 0$ until a predefined number L **do**
4:        $\nu(l) \Longleftarrow l$ mod N
5:        **if** $\boldsymbol{\theta}_p^l \in \mathcal{D}_{\nu(l)}$ **then**
6:           $\boldsymbol{\theta}_p^{l+1} \Longleftarrow \boldsymbol{\theta}_p{}^l$
7:        **else**
8:           $\mathcal{P}_{\mathcal{D}_{\nu(l)}}(\boldsymbol{\theta}_p^l) \Longleftarrow \frac{\boldsymbol{\theta}_p - \mathbf{z}_{\nu(l)}}{\|\boldsymbol{\theta}_p^l - \mathbf{z}_{\nu(l)}\|} \hat{r}_{\nu(l)}$
9:           $\boldsymbol{\theta}_p^{l+1} \Longleftarrow (1 - \lambda_l)\boldsymbol{\theta}_p{}^l + \lambda_l \mathcal{P}_{\mathcal{D}_{\nu(l)}}(\boldsymbol{\theta}_p{}^l)$
10:        **end if**
11:     **end for**
12:     **for** $j = 0$ until a predefined number J **do**
13:        $\nu(j) \Longleftarrow j$ mod NM
14:        **if** $\boldsymbol{\theta}_s^j \in \mathcal{E}_{\nu(j)}$ **then**
15:        $\boldsymbol{\theta}_s^{j+1} \Longleftarrow \boldsymbol{\theta}_s{}^j$
16:        **else**
17:           $\boldsymbol{\theta}_T \Longleftarrow \left[\mathbf{F}_{\nu(j)} \begin{bmatrix} \boldsymbol{\theta}_s^j \\ 1 \end{bmatrix} \right]_{2 \times 1}$
18:           $\mathcal{P}_{\mathcal{E}_{\nu(j)}}(\boldsymbol{\theta}_s^j) \Longleftarrow \left[\mathbf{F}_{\nu(j)}^{-1} \begin{bmatrix} \frac{\boldsymbol{\theta}_T}{\|\boldsymbol{\theta}_T\|} \\ 1 \end{bmatrix} \right]_{2 \times 1}$
19:           $\boldsymbol{\theta}_s^{j+1} \Longleftarrow (1 - \lambda_j)\boldsymbol{\theta}_s{}^j + \lambda_j \mathcal{P}_{\mathcal{E}_{\nu(j)}}(\boldsymbol{\theta}_s{}^j)$
20:        **end if**
21:     **end for**
22:     $\boldsymbol{\theta}_k = \left(\boldsymbol{\theta}_c^{L+1} + \boldsymbol{\theta}_s^{J+1} \right) / 2$
23:     $\boldsymbol{\theta}_p^0 = \boldsymbol{\theta}_k$ and $\boldsymbol{\theta}_s^0 = \boldsymbol{\theta}_k$
24: **end for**

convex set. The estimation accuracy can be improved by combining the two estimates, namely by computing the average and using it as a new initial value. This procedure continues for a certain number of iterations. Algorithm 2 shows the modified version of POCS in cooperative mode (CE-POCS2).

In both algorithms, $\{\lambda_k\}_{k=0}^{\infty}$ are relaxation parameters. In the simulations, the relaxation parameters are first set to one, and after a given number k_0 iterations, they decrease as

$$\lambda_k = \left\lceil \frac{k - k_0 + 1}{N} \right\rceil^{-1}, \tag{29}$$

where $\lceil x \rceil$ denotes the smallest integer greater than or equal to x.

IV. SIMULATION RESULTS

We consider a 100×100 square area. To set reasonable values for the variances of TOA estimation errors, we consider the Cramér-Rao lower bound (CRLB). Suppose that we are using a signal with $2\,\text{MHz}$ null-to-null bandwidth with rectangular pulse shaping. The CRLB for the TOA estimation is given by [9]

$$\sqrt{\text{var}(\hat{r}_i)} \geq \frac{c}{2\sqrt{2}\pi\sqrt{\text{SNR}}\,\xi}, \tag{30}$$

where SNR is the signal-to-noise ratio and ξ is the effective bandwidth, which is defined as follows [10],

$$\xi = \left[\frac{\int_{-\infty}^{\infty} f^2 |S(f)|^2 df}{\int_{-\infty}^{\infty} |S(f)|^2 df} \right]^2. \tag{31}$$

For the noise spectral density, $N_0 = 10^{-12}\text{W/Hz}$ is considered.

To compute the SNR, we need the ensemble mean power at the ith node, measured in dB, which can be modeled as [11]

$$P_i = P_0 - 10\beta \log_{10}\left(\frac{r_i(\boldsymbol{\theta})}{d_0}\right) + w_{P_i}, \tag{32}$$

where β is a path-loss factor and P_0 is the received power in dBm at a calibration distance d_0. Variable w_{P_i} is a log-normal shadowing term, i.e, $w_{P_j} \sim \mathcal{N}(0, \sigma_{P_i}^2)$. In the simulations, we set the following values for different parameters in (32):

$$\beta = 2.5, \ P_0 = -70\,\text{dBm}, \ d_0 = 1\text{m}, \ \sigma_{P_i}^2 = \sigma_P^2 = 4\,\text{dB}^2.$$

The cumulative distribution function (CDF) is used to compare the performance of the different methods. The performance of the POCS approach is compared with the MLE derived in [5]. We use the same network deployment as in [5], where four reference nodes are located at the corners of the square area. To investigate the performance of the proposed method, we consider two cases as in [5]. In one case, three reference nodes are to be the PRNs and the remaining last one plays as the SRN. In the second case, two nodes on two non-consecutive vertices of the square area are the PRNs and the two other nodes are the SRNs. The target is randomly placed inside the square area over a grid of 19×19. For algorithm 2, the procedure is repeated for five iterations. To implement the MLE, Matlab's gradient-based `lsqnonlin` routine [12] is used.
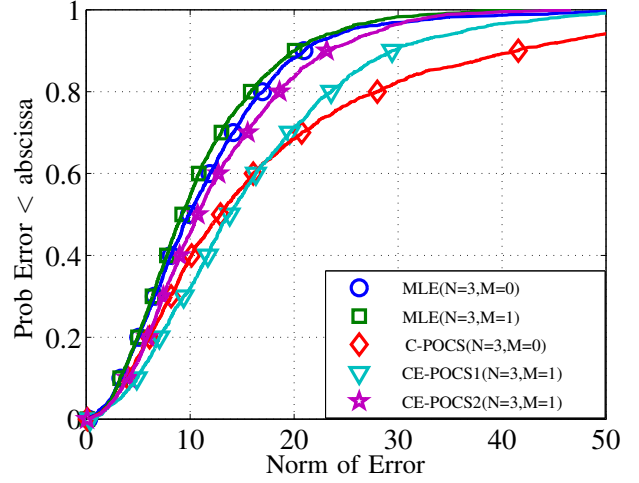

Fig. 3: CDF of cooperative and non-cooperative MLE and POCS for TW-TOA/TDOA measurements (a) $N = 3$, $M = 0$, and (b) $N = 3$, $M = 1$.
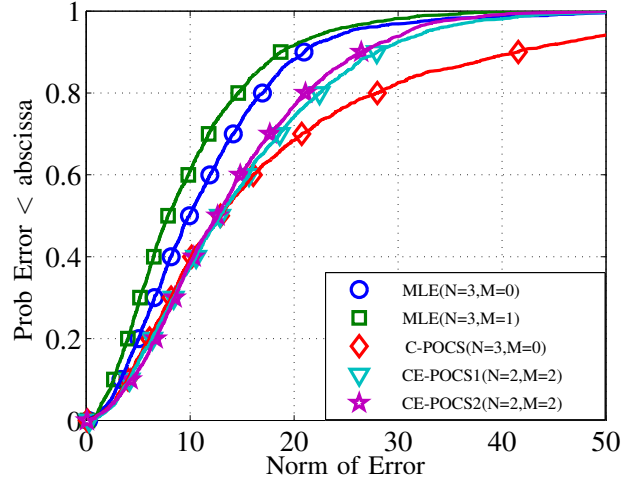

Fig. 4: CDF of cooperative and non-cooperative MLE and POCS for TW-TOA/TDOA measurements (a) $N = 3$, $M = 0$, and (b) $N = 2$, $M = 2$.

Fig. 3 shows the CDFs of the positioning errors for the MLE and POCS methods. It is clear that the MLE in cooperation mode shows good performance compared to the other methods. It only converges in a small percentage of cases to local minima resulting in large errors. It is also seen that cooperation can improve the performance of CE-POCS for large measurement errors. For this network, we can see that the second algorithm with five iterations improves CE-POCS such that it becomes comparable to the MLE. Another important observation is that the gain obtained in the POCS approach due to cooperation is significantly greater than that of the MLE.

Fig. 4 shows the CDF for cooperative and non-cooperative algorithms in the second case, where the network contains two

PRNs and two SRNs. Again the figure shows that cooperation improves the performance of both the MLE and POCS. For the POCS approach, the improvements for large errors are higher than those for the MLE. It also shows that algorithms 2 and 1 approximately give the same performance. In other simulations, we have observed that algorithm 2 often outperforms algorithm 1.

V. Conclusion

In this paper we have studied the positioning problem in cooperative networks with both active and passive sensors. An MLE can be derived based on measurements in different nodes and an iterative search can be employed to solve it. However, due to the nonlinear cost function of the MLE, it needs a good initialization, which increases the computational complexity. Using a geometric interpretation, we have formulated the positioning problem as finding the intersection of a number of convex sets. The proposed method is a robust technique and can be implemented in a fully distributed manner. Simulation results indicate a good performance for the proposed method.

References

[1] R. Huang and G. Zaruba, "Beacon deployment for sensor network localization," in *IEEE Wireless Communications and Networking Conference*, March 2007, pp. 3188–3193.

[2] A. Sayed, A. Tarighat, and N. Khajehnouri, "Network-based wireless location: challenges faced in developing techniques for accurate wireless location information," *IEEE Signal Processing Magazine*, vol. 22, no. 4, pp. 24–40, July 2005.

[3] C. Chang and A. Sahai, "Cramér-Rao-type bounds for localization," *EURASIP Jounal on Applied Signal Processing*, no. 1, pp. 166–166, 2006.

[4] M. Rydström, "Algorithms and models for positioning and scheduling in wireless sensor networks," Ph.D. dissertation, Chalmers University of Technology, 2008.

[5] S. Gezici and Z. Sahinoglu, "Enhanced position estimation via node cooperation," in *Proc. IEEE International Conference on Communications (ICC)*, May 2010, Available:~www.ee.bilkent.edu.tr/~gezici/ICC10.pdf.

[6] R. Fujiwara, K. Mizugaki, T. Nakagawa, D. Maeda, and M. Miyazaki, "TOA/TDOA hybrid relative positioning system using UWB-IR," in *IEEE Radio and Wireless Week*, January 2009, pp. 679–682.

[7] H. Wymeersch, J. Lien, and M. Win, "Cooperative localization in wireless networks," *Proceedings of the IEEE*, vol. 97, no. 2, pp. 427–450, February 2009.

[8] I. Ihrke, "Some notes on ellipse," 2004, http://people.cs.ubc.ca/~ivoihrke/software/ellipse.pdf.

[9] S. Gezici, "A survey on wireless position estimation," *Wireless Personal Communications (Special Issue on Towards Global and Seamless Personal Navigation)*, vol. 44, no. 3, pp. 263–282, Februray 2008.

[10] S. Gezici, Z. Tian, G. Giannakis, H. Kobayashi, A. Molisch, H. Poor, and Z. Sahinoglu, "Localization via ultra-wideband radios: A look at positioning aspects for future sensor networks," *IEEE Signal Processing Magazine*, vol. 22, no. 4, pp. 70–84, July 2005.

[11] N. Patwari, J. Ash, S. Kyperountas, A. Hero, and N. Correal, "Locating the nodes: Cooperative localization in wireless sensor network," *IEEE Signal Processing Magazine*, vol. 22, no. 4, pp. 54–69, July 2005.

[12] The Mathworks Inc., "On-line," http://www.mathworks.com, 2010.